

NUMERICAL INVESTIGATIONS OF HEAT TRANSFER IN PHASE CHANGE MATERIALS (PCMS) USING NON-THERMAL EQUILIBRIUM MODEL

Y. Tian, C.Y. Zhao*

School of Engineering, University of Warwick, CV4 7AL, United Kingdom

*Email: C.Y.Zhao@warwick.ac.uk

ABSTRACT

Phase change materials (PCMs) are drawing increasing attention of researchers nowadays, and they play a pivotal role in thermal energy storage (TES) used in renewable energy resources applications, since these renewable energy, such as solar energy, wind energy and tidal energy, are intermittent and not available at any time. However, most of PCMs suffer from low thermal conductivities prolonging the charging and discharging processes.

Metal foams with relatively high thermal conductivities, are believed to be able to enhance heat transfer performance of PCMs for those applications. In this paper, a two-equation non-thermal equilibrium model has been employed to tackle the phase change heat transfer problem in PCMs composites embedded into metal foams. Numerical results show good agreement with experimental data, and indicate that a better heat transfer performance can be achieved by using the metal foams of smaller pore size and smaller porosity, and heat transfer performance of PCMs can be enhanced by up to 10 times by embedded metal foams into PCMs.

KEYWORDS

Heat transfer enhancement; PCMs; Metal foams; Porosity; Pore size; Two-equation model; Non-thermal equilibrium; Charging process;

INTRODUCTION

Fossil fuels, which have brought great convenience to human being, have been used extensively in the past centuries since the Industrial Revolution. However, CO₂ emissions during burning fossil fuels have caused global warming, and they have been an imminent issue to be tackled nowadays, so it is necessary for us to find reliable solutions to reduce CO₂ emissions. Renewable energy resources are now regarded as a promising way for curbing the global warming and for sustainable development, but these energy resources such as solar energy and wind energy, are intermittent and obviously there is an inevitable time discrepancy between the energy demand and energy generation. Consequently, thermal energy storage (TES) [1] technologies undoubtedly play a pivotal role in many renewable energy resources applications. Phase change materials (PCMs) [1], as a sort of functional materials used in TES, they release or absorb thermal energy during melting and solidification processes. Many previous researchers [2-4] have investigated PCMs in many aspects, such as solar power plants [5], industrial waste heat recovery [6], high-efficient compact heat sink [7], solar cooker [8] and building applications [9-11].

However, most PCMs suffer from the common problem of low thermal conductivities, being around 0.2 and 0.5 for paraffin wax and inorganic salts respectively, which prolongs the charging and discharging period. Therefore, a heat transfer enhancement technology in PCMs is needed [12,13]. Under these circumstances, metal foams [14-23], as a sort of novel material with high strength-to-density ratio, ultralight porous structure and relatively high thermal conductivity, are believed to be a promising material for enhancing heat transfer performance of PCMs.

This paper presents a two-dimensional thermal analysis of PCMs embedded inside metal foams. A two-equation non-thermal equilibrium model is employed in this paper for counting the temperature difference between metal ligaments and PCMs. The results show that the non-thermal equilibrium model based on two-equation conception shows good agreement with experimental data.

PHYSICAL PROBLEM

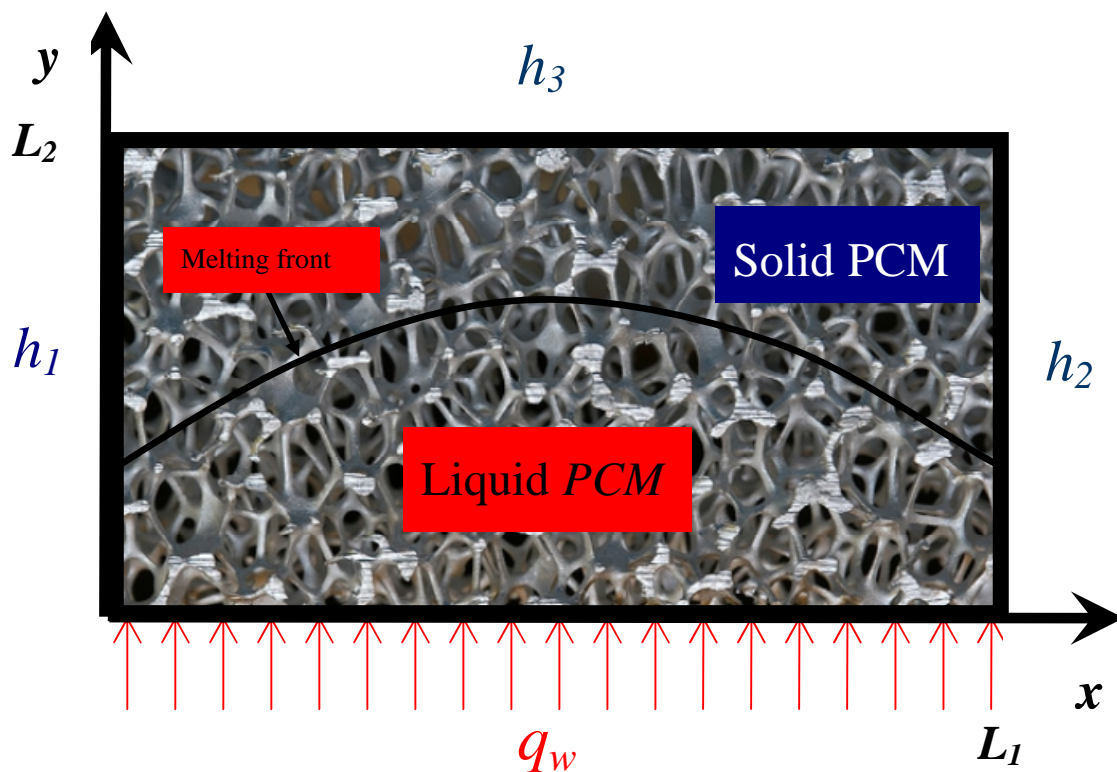


Fig. 1 PCMs embedded into metal foams

As is shown in Fig. 1, PCMs (paraffin wax is used in this study) are encapsulated in rectangular metal foams

made of copper. The lengths of the sample are L_1 in x-direction and L_2 in y-direction. PCMs and metal foams are heated on the bottom side through a constant heat flux q_w provided by an electric heater, and the three other boundaries (left, right and top side) are placed in the atmosphere and incur heat loss into the air, where the heat transfer coefficients are h_1 , h_2 and h_3 respectively.

GOVERNING EQUATIONS

With natural convection being neglected, the two-equation non-thermal equilibrium model can be obtained as follows:

$$(1-\varepsilon) \frac{\partial T_s(x, y, t)}{\partial t} = \alpha_{se} \left[\frac{\partial^2 T_s(x, y, t)}{\partial x^2} + \frac{\partial^2 T_s(x, y, t)}{\partial y^2} \right] - \frac{k_{int}}{\rho_s C_{ps}} a_{sf} \frac{[T_s(x, y, t) - T_f(x, y, t)]}{d} \quad (1)$$

$$\varepsilon \frac{\partial T_f(x, y, t)}{\partial t} = \alpha_{fe} \left[\frac{\partial^2 T_f(x, y, t)}{\partial x^2} + \frac{\partial^2 T_f(x, y, t)}{\partial y^2} \right] + \frac{k_{int}}{\rho_f C_{pf}} a_{sf} \frac{[T_s(x, y, t) - T_f(x, y, t)]}{d} \quad (2)$$

$$T_s(x, y, 0) = T_f(x, y, 0) = T_0 \quad (3)$$

$$k_{se} \frac{\partial T_s(x, 0, t)}{\partial y} + k_{fe} \frac{\partial T_f(x, 0, t)}{\partial y} = -q_w \quad (4)$$

$$T_f(x, 0, t) = T_s(x, 0, t) \quad (5)$$

$$T_f[S_x(y, t), S_y(x, t), t] = T_m \quad (6)$$

$$k_{se} \frac{\partial T_s(0, y, t)}{\partial x} + h_1(1-\varepsilon)[T_\infty - T_s(0, y, t)] = 0 \quad (7)$$

$$k_{fe} \frac{\partial T_f(0, y, t)}{\partial x} + h_1\varepsilon[T_\infty - T_f(0, y, t)] = 0 \quad (8)$$

$$-k_{se} \frac{\partial T_s(L_1, y, t)}{\partial x} + h_2(1-\varepsilon)[T_\infty - T_s(L_1, y, t)] = 0 \quad (9)$$

$$-k_{fe} \frac{\partial T_f(L_1, y, t)}{\partial x} + h_2\varepsilon[T_\infty - T_f(L_1, y, t)] = 0 \quad (10)$$

$$-k_{se} \frac{\partial T_s(x, L_2, t)}{\partial y} + h_3(1-\varepsilon)[T_\infty - T_s(x, L_2, t)] = 0 \quad (11)$$

$$-k_{fe} \frac{\partial T_f(x, L_2, t)}{\partial y} + h_3\varepsilon[T_\infty - T_f(x, L_2, t)] = 0 \quad (12)$$

Note:

Eq. (3): initial conditions when $t=0$

Eq. (4) and Eq. (5): boundary conditions at $y=0$ (the bottom side which is subject to constant heat flux)

Eq. (6): boundary condition at $x=S(x, y, t)$ (melting front)

Eq. (7) and Eq. (8): boundary conditions at $x=0$ (left boundary)

Eq. (9): Eq. (10): boundary conditions at $x=L_1$ (right boundary)

Eq. (11): Eq. (12):: boundary conditions at $y=L_2$ (top side)

The above equations can be solved only if $S(x, y, t)$ has been given, unfortunately it is unlikely for us to obtain $S(x, y, t)$ beforehand. The function, $S(x, y, t)$, which stands for moving melting boundary, is being coupled with $T(x, y, t)$. The correlation between $S(x, y, t)$ and $T(x, y, t)$ is given by Eq. (13) and Eq. (14), which can be obtained by the Energy Conservation Law.

$$\rho H_L \varepsilon \frac{d(S_x(y,t))}{dt} = k_{fe} \frac{\partial T_f(S_x(y,t)^+, y, t)}{\partial x} - k_{fe} \frac{\partial T_f(S_x(y,t)^-, y, t)}{\partial x} + k_{int} a_{sf} \frac{d(S_x(y,t))}{dt} \frac{T_s[S_x(y,t), y, t] - T_f[S_x(y,t), y, t]}{d} \quad (13)$$

$$\rho H_L \varepsilon \frac{d(S_y(x,t))}{dt} = k_{fe} \frac{\partial T_f(x, S_y(x,t)^+, t)}{\partial y} - k_{fe} \frac{\partial T_f(x, S_y(x,t)^-, t)}{\partial y} + k_{int} a_{sf} \frac{d(S_y(x,t))}{dt} \frac{T_s[x, S_y(x,t), t] - T_f[x, S_y(x,t), t]}{d} \quad (14)$$

In Eq. (13) and Eq. (14), the superscript “+” means the Right Limit in Mathematics, representing solid zone of PCMs, while the superscript “-” means the Left Limit in Mathematics, representing fluid zone of PCMs. Wherein Eq. (13) and Eq. (14) denote x-component and y-component of melting front function respectively.

With regard to the complicated microstructures in metal foams, a three-dimensionally structured model (tetrakaidecahedron) presented by Boomsma and Poulikakos [15] has been used to deal with the effective thermal conductivity of metal foams. In addition, some important geometrical parameters of metal foams, such as specific surface area, pore size and metal fiber diameter, still need to be resolved. In order to do this, Calmidi’s model [14] is employed in this study.

NUMERICAL PROGRAMME

A FDM-based (Finite Difference Method) programme has been developed for dealing with the phase change heat transfer problem in PCMs embedded into metal foams aforementioned. The uniform mesh grids are employed in this study, and they are $14 \times 112 \times 6000$, i.e. 14 for spatial grids of y-direction (0.025 m), 112 for spatial grids of x-direction (0.2 m) and 6000 for time grids. Iterations are aborted when the maximum difference between two successive iterations is smaller than 10^{-6} .

RESULTS AND DISCUSSIONS

Comparisons with experimental data

The numerical results are compared with the corresponding experimental data. In the experiment, a piece of rectangular metal foam (200x120x25 mm in dimension, copper foam of 10 ppi and 95% porosity) was embedded in RT58 (melting temperature: 48-62°C, latent heat of fusion: 181 kJ/kg, according to the PCMs provider RUBITHERM®).

Fig. 2 shows a comparison between numerical results and experimental data. The y denotes the vertical coordinate of the computational domain, meaning the distance from different locations to heating wall. Both numerical results and experimental data show that PCMs begin to melt around $t = 1200$ s and finish phase change around $t = 4000$ s, and a good agreement between them has been achieved. It needs to be noticed that the PCMs we used in this experiment are not a sort of proper crystal material which has fixed melting point, this RT58 melts in a temperature range of 48-62°C. However in our numerical investigations, PCMs are regarded as a sort of phase change materials which have constant melting point. This makes it impossible to achieve a perfect agreement between numerical results and experimental data, unless the PCMs with fixed melting point are used. As is shown in Fig. 2 the temperatures of RT58 increase more slowly than before, this is because the heat provided is mainly used for phase change not for sensible heat increasing. After RT58 has fully become liquid state when temperatures are higher than 62°C, its temperatures begin to increase faster again, this is because the heat provided is not used for overcoming latent heat of fusion any more, and only for sensible heat increasing of PCMs. Whilst numerical results indicate that PCMs melt at constant temperature (melting point: 58°C), which is different from experimental data, this is because RT58 used in this experiment is not proper crystal material and has not fixed melting point.

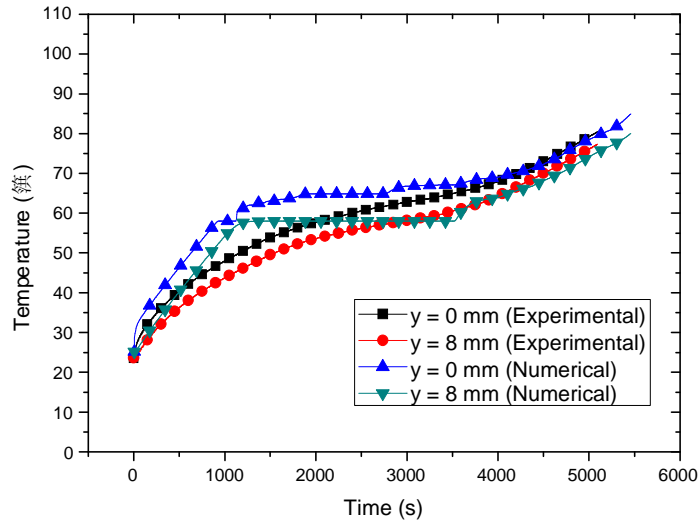


Fig. 2 Results of two-equations model compared with experimental data

Effects of metal foam parameters on heat transfer

Fig. 3 shows a comparison of temperature differences among 3 metal foam samples with different porosities and pore sizes (10 ppi, 95% porosity; 30 ppi, 95% porosity; 30 ppi, 85% porosity respectively). These temperature differences denote the temperature differences between $y = 0 \text{ mm}$ (wall) and $y = 8 \text{ mm}$, which reflect heat transfer performance when an uniform heat flux is imposed on the boundary (smaller temperature differences mean better heat transfer). It can be seen clearly that the temperature differences in the metal foam samples with smaller porosities and pore sizes are much smaller than those in the metal foam samples with bigger porosities and pore sizes, this is because the metal foams with smaller pore sizes (30 ppi) have bigger specific surface area than those with bigger pore sizes (10 ppi). Therefore in the case of the former, the metal ligaments have bigger contact area with PCMs so that these ligaments can transfer more heat to PCMs which leads to smaller temperature differences between metal ligaments and PCMs in the former than those in the latter.

From Fig. 3, it can be also clearly seen that the metal foams with smaller porosities (85%) have smaller temperature differences than those with bigger porosities (95%), and hence the former can achieve better heat transfer performance than the latter. This is because that there are more metal skeletons used for transferring heat to PCMs in the former than in the latter.

In Fig. 3, the temperature differences keep steady at the beginning, and plummet suddenly around $t = 1200 \text{ s}$, this is because that at this moment melting begins and this phase change phenomenon enhances heat transfer performance. As time goes on and melting continues, the temperature differences stay relatively stable for a period. When $t = 2500 \text{ s}$ more or less, the temperature differences rise again, this is because that the PCMs near heating wall have finished absorbing latent heat of fusion for melting process and their temperatures rise dramatically after phase change during melting, whilst at this moment, the PCMs at $y = 8 \text{ mm}$ have not finished phase change process and they still keep a constant temperature of 58°C . As time goes on, the part of PCMs at $y = 8 \text{ mm}$ has finished phase change process and consequently their temperatures rise dramatically around $t = 3000 \text{ s}$, which leads to a decrease in the temperature differences between the PCMs at $y = 0 \text{ mm}$ (wall) and $y = 8 \text{ mm}$. More and more PCMs have finished their phase change processes as time elapses, and all PCMs have become liquid state around $t = 4500 \text{ s}$. So after that phase change phenomenon is not taking place any more, and it will have been a simplex liquid heat transfer problem after $t = 4500 \text{ s}$, this is just the reason why the aforementioned temperature differences keep stable again after $t = 4500 \text{ s}$.

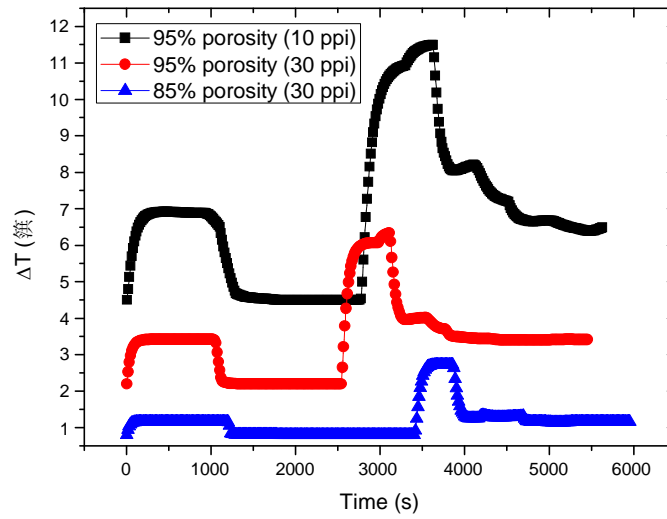


Fig. 3 A comparison of temperature differences among different porosities and pore sizes

Comparison with the case without metal foams

Fig. 4 compares PCMs which are embedded into metal foams with the case of PCMs without metal foams, and it clearly shows that the temperature differences in PCMs without metal foams are much bigger than PCMs embedded into metal foams (about 10 times bigger than the latter). That is to say that PCMs embedded into metal foams have up to 10 times heat transfer performance of the case without metal foams, meaning that heat transfer in PCMs undoubtedly can be enhanced significantly by using metal foams, and metal foams being embedded into PCMs can be a good solution for accelerating the charging and discharging processes of PCMs, which is quite helpful when stored thermal energy in solar power plants is needed to be released for electricity producing. It still needs to be noticed that natural convection in PCMs is not considered in this study, so in practical applications, temperature difference in pure PCMs will not be as big as that shown in Fig. 4. In addition, it can be seen from Fig. 4 that the temperatures of PCMs with metal foam are in the middle of those temperatures of PCMs without metal foam, which reflects energy conservation (the same heat flux provided).

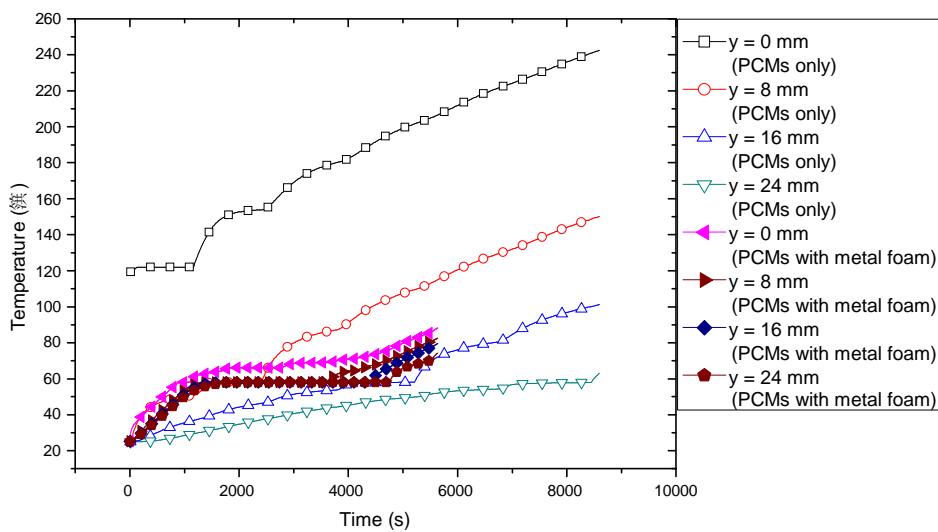


Fig. 4 A comparison between PCMs embedded into metal foam and PCMs only

CONCLUSIONS

In this paper, a numerical investigation based on two-equation non-equilibrium heat transfer model has been carried out to tackle the phase change heat transfer problem in PCMs embedded into metal foams. The numerical results based on two-equation non-thermal equilibrium model show a good agreement with experimental data, although the PCMs (RT58) used in experiment are not a sort of proper crystal material with fixed melting point. Numerical results show that the metal foams of smaller pore size and smaller porosity can achieve better heat transfer performance than those of bigger pore size and bigger porosity. The numerical results are compared with the case without metal foams, and it is shown that the addition of metal foams can dramatically reduce the temperature difference of the PCMs through the heat conduction of metal foam structures embedded in the whole domain, and thereby significantly enhancing the heat transfer by up to ten times compared with pure PCMs .

ACKNOWLEDGEMENTS

This work is supported by the UK Engineering and Physical Science Research Council (EPSRC grant number: EP/F061439/1) and Warwick Research Development Fund (RDF) Strategic Award (RD07110).

NOMENCLATURE

q_w	heat flux
T_m	fusion temperature
T_0	initial temperature
T_f	temperature of surrounding fluids
H_L	latent heat of fusion
C_p	specific heat of fluid at constant pressure
C_{ps}	specific heat of metal at constant pressure
k	thermal conductivity
k_s	thermal conductivity of metal ligament
k_f	thermal conductivity of fluid
k_e	effective thermal conductivity
k_{fe}	effective thermal conductivity without metal
k_{se}	effective thermal conductivity without fluid
k_{int}	interstitial thermal conductivity
L_1	length of PCMs sample in x -axis
L_2	length of PCMs sample in y -axis
x	coordinate of location (x -component)
y	coordinate of location (y -component)
t	time
t_{ref}	reference time
$T(x, y, t)$	temperature function
$S(x, y, t)$	profile function of melting front
$S_x(y, t)$	x -component of $S(x, y, t)$
$S_y(x, t)$	y -component of $S(x, y, t)$
h_1	heat transfer coefficients at the left boundary
h_2	heat transfer coefficients at the right boundary
h_3	heat transfer coefficients at the top boundary

Subscripts

x	x -component of certain function
y	y -component of certain function
s	metal ligament
f	fluid (PCMs)

Superscripts

*	dimensionless parameters
+	right limit of certain function
-	left limit of certain function

Greek

ρ	density
α	thermal diffusivity
ε	porosity
λ	ratio of ligament radius to ligament length
τ	increment of t

REFERENCES

- [1] B. Zalba, J. M. Marin, L. F. Cabeza, and H. Mehling, Review on thermal energy storage with phase change: materials, heat transfer analysis and applications, *Appl. Therm. Eng.* 23 (2003) 251-283.
- [2] A. A. El-Sebaei, A. A. Al-Ghamdi, F. S. Al-Hazmi, A. S. Faidah, Thermal performance of a single basin solar still with PCM as a storage medium, *Appl. Energ.* 86 (2009) 1187-1195.
- [3] A. Najjar, A. Hasan, Modeling of greenhouse with PCM energy storage, *Energ. Convers. Manage.* 49 (2008) 3338-3342.
- [4] V. V. Tyagi, D. Buddhi, Thermal cycle testing of calcium chloride hexahydrate as a possible PCM for latent heat storage, *Sol. Energ. Mat. Sol. C.* 92 (2008) 891-899.
- [5] H. Michels, R. Pitz-Paal, Cascaded latent heat storage for parabolic trough solar power plants, *Solar Energy* 81 (2007) 829-837.
- [6] D. Buddhi, Thermal performance of a shell and tube PCM storage heat exchanger for industrial waste heat recovery, Presented at solar world congress, Taejon, Korea, August 24th – 30th, 1977.
- [7] V. Shatikian, G. Ziskind, R. Letan, Numerical investigation of a PCM-based heat sink with internal fins: Constant heat flux, *Int. J. Heat Mass Transfer* 51 (2008) 1488-1493.
- [8] S. D. Sharma, T. Iwata, H. Kitano, K. Sagara, Thermal performance of a solar cooker based on an evacuated tube solar collector with a PCM storage unit, *Solar Energy* 78 (2005) 416-426.
- [9] I. O. Salyer, A. K. Sircar, Phase change materials for heating and cooling of residential buildings and other applications, *Proceedings of 25th Intersociety Energy Conversion Engineering Conference* 1990 236–43.
- [10] D.A. Neeper, Thermal dynamics of wallboard with latent heat storage, *Solar Energy* 68 (2000) 393–403.
- [11] A.K. Athienitis, C. Liu, D. Hawes, D. Banu, D. Feldman, Investigation of the thermal performance of a passive solar test-room with wall latent heat storage. *Build. Environ.* 32 (1997) 405–410.
- [12] E.S. Mettawee and G.M.R. Assassa, Thermal Conductivity enhancement in a Latent Heat Storage System, *Solar Energy* 81 (2007) 839-845.
- [13] A. Mills, M. Farid, J. R. Selmán, S. Al-Hallaj, Thermal conductivity enhancement of phase change materials using a graphite matrix, *Appl. Therm. Eng.* 26 (2006) 1652-1661.
- [14] V. V. Calmidi, Transport Phenomena in High Porosity Metal Foams, Ph.D thesis, University of Colorado 1998.
- [15] K. Boomsma, D. Poulikakos, On the effective thermal conductivity of a three-dimensionally structured fluid-saturated metal foam, *Int. J. Heat Mass Transfer* 44 (2001) 827 – 836.
- [16] A. Bhattacharya, V. V. Calmidi, and R. L. Mahajan, Thermophysical properties of high porosity metal foams, *Int. J. Heat Mass Transfer* 45 (2002) 1017-1031.
- [17] M. S. Phanikumar, R. L. Mahajan, Non-Darcy natural convection in high porosity metal foams, *Int. J. Heat Mass Transfer* 45 (2002) 3781-3793.
- [18] W. Lu, C. Y. Zhao, S. A. Tassou, Thermal Analysis on Metal-Foam Filled Heat Exchangers, Part I: Metal-Foam Filled Pipes, *Int. J. Heat Mass Transfer* 49 (2006) 2751-2761.

- [19] C. Y. Zhao, T. Kim, T. J. Lu, and H. P. Hodson, Thermal transport in high porosity cellular metal foams, *Journal of Thermophysics and Heat Transfer* 18 (2004) 309-317.
- [20] C. Y. Zhao, T. J. Lu, H. P. Hodson, Natural convection in metal foams with open cells, *Int. J. Heat Mass Transfer* 48 (2005) 2452-2463.
- [21] C. Y. Zhao, T. J. Lu, H. P. Hodson, Thermal radiation in ultralight metal foams with open cells, *Int. J. Heat Mass Transfer* 47 (2004) 2927-2939.
- [22] S. Krishnan, J. Y. Murthy, S. V. Garimella, A two-temperature model for solid-liquid phase change in metal foams, *ASME J. Heat Transfer* 127 (2005) 995-1004.
- [23] Y. Tian, C.Y. Zhao, Heat transfer analysis for phase change materials (PCMs), The 11th International Conference on Energy Storage (Effstock 2009) , Stockholm, Sweden.